Biochem. J. (1991) 279, 711–718 (Printed in Great Britain)

Regulation of the acto·myosin subfragment 1 interaction by troponin/tropomyosin

Evidence for control of a specific isomerization between two acto·myosin subfragment 1 states

Daniel F. A. McKILLOP* and Michael A. GEEVES
Department of Biochemistry, School of Medical Sciences, University of Bristol, University Walk, Bristol BS8 1TD, U.K.
Bristol BS8 1TD, U.K.

The co-operative binding of myosin subfragment 1 (S1) to reconstituted skeletal-muscle thin filaments has been examined by monitoring the fluorescence of a pyrene probe on Cys-374 of actin. The degree of co-operativity differs when phosphate, sulphate or ADP are bound to the S1 active site. Binding isotherms have been analysed according to the Geeves & Halsall [(1987) Biophys. J. **52**, 215–220] model, which proposed that troponin and tropomyosin effected regulation of the actomyosin interaction by controlling an isomerization of the actomyosin complex. The data support the proposal that seven actin monomers associated with a single tropomyosin molecule act as a co-operative unit that can be in one of two states. In the 'closed' state myosin can bind to actin, but the subsequent isomerization is prevented. The isomerization is only allowed after the seven-actin unit is in the 'open' form. Ca^{2+} controls the proportion of actin filaments in the 'closed' and 'open' forms in the absence of myosin heads. The ratio of 'closed' to 'open' forms is approx. 50:1 in the absence of Ca^{2+} and 5:1 in its presence.

INTRODUCTION

Tropomyosin (Tm) and troponin (Tn) are the proteins responsible for the Ca^{2+} regulation of the interaction between actin of the thin filaments and myosin in vertebrate straited muscle [1]. In the absence of Tn/Tm, myosin and its proteolytic subfragments, subfragment 1 (S1) and heavy meromyosin (HMM), bind to actin with no measurable co-operativity [2]. In the presence of Tn/Tm myosin binds to actin with positive co-operativity [3]. This co-operative binding is present both in the presence and in the absence of Ca^{2+}, but the degree of co-operativity is greater in the absence of Ca^{2+}.

Hill *et al.* [4] proposed a model for the co-operative binding of myosin to actin. In this model the co-operative unit is seven actin monomers bridged by a single Tm molecule (A_7·Tm). This co-operative unit can exist in two states, which are in equilibrium. These were originally called the 'weak' and 'strong' states, but are referred to here as the 'off' and 'on' states to distinguish them from the 'weak' and 'strong' myosin states referred to below. Myosin binds weakly to A_7·Tm units in the 'off' state, but much more strongly to them in the 'on' state. Binding of a single myosin head to an A_7·Tm unit can switch it to the 'on' state, resulting in co-operative myosin binding. An additional source of co-operativity was attributed to nearest-neighbour interaction between A_7·Tm units.

The affinity of myosin for actin is dependent on the nucleotide bound at the myosin ATPase site. Myosin·nucleotide complexes have been classed as either weak (M·ATP, M·ADP·P_i) or strong (M, M·ADP) actin-binding complexes [2]. The degree of co-operativity observed is related to the nucleotide bound to the myosin, with only 'strong' binding complexes showing co-operative binding to regulated actin. A modification of the co-operative scheme of Hill *et al.* [4] was proposed by Geeves & Halsall [5]. This was based on a model for the interaction of actin and myosin proposed by Geeves *et al.* [6] and demonstrated by observations from our laboratory that the binding of S1 to actin involved at least two steps following the formation of the collision complex [7]:

$$A + M \overset{K_0}{\rightleftharpoons} \{AM\} \overset{K_1'}{\rightleftharpoons} A\text{–}M \overset{K_2}{\rightleftharpoons} A \cdot M$$

The formation of the collision complex ({AM}) cannot be detected spectroscopically, and therefore the formation of A–M is treated as one step and K_1 refers to $K_0 \cdot K_1'$. We refer to the two states as the A-state ('attached') and the R-state ('rigor-like'). 'Strong' myosin states were those in which $K_2 > 1$ and 'weak' myosin states were those in which $K_2 < 1$. In the original model presented by Geeves *et al.* [6] it was proposed that Tn/Tm could control myosin binding to actin by controlling the first-order isomerization step from the 'attached' to the 'rigor-like' state. The Geeves & Halsall model [5] was a formalization of this proposal, and is related to the Hill *et al.* model [4] in that the weak binding constant is K_1 and the strong binding constant is $K_1 \cdot (1 + K_2)$. The two A_7·Tm states in the Geeves & Halsall model were described as the 'open' and 'closed' states. In the present paper the terms 'on' and 'off' are used to describe regulatory states independent of model, and 'closed' and 'open' refer to states with the characteristics attributed in the Geeves & Halsall model. The equilibrium constant K_T defines the ratio of A_7·Tm units in the 'closed' and 'open' states and is equivalent to the inverse of the parameter L in the Hill *et al.* model. The Geeves & Halsall model did not consider nearest-neighbour interaction between co-operative units.

A feature of the Geeves & Halsall model is that K_1 and K_2 are independent of the presence of Ca^{2+}, only K_T being affected by Ca^{2+}. K_1 and K_2 are dependent upon the nucleotide bound to myosin, but K_T is independent of nucleotide. Therefore K_1 and K_2 can be measured in the presence of Ca^{2+} for a range of myosin·nucleotide or myosin·nucleotide analogue states as shown previously [8]. These measured constants are independent

Abbreviations: Tm, tropomyosin; Tn, troponin; S1, myosin subfragment 1; HMM, heavy meromyosin; A, actin; M, myosin; pyr-actin, pyrene-labelled actin; Ap_5A, P^1P^5-di(adenosine-5′-)pentaphosphate; τ, relaxation time; overbars indicate free concentrations.

* To whom correspondence should be addressed.

of the co-operative model, but the model then predicts that the myosin binding isotherm will be defined by K_T. K_T will be dependent upon the presence of Ca^{2+} but its value will be independent of the nucleotide bound to myosin. In the work reported here, we test this hypothesis by measuring myosin binding isotherms in the absence of any nucleotide, and in the presence of ADP, phosphate and sulphate, all of which bind to the myosin ATPase site and change both K_1 and K_2 in unregulated actin [9,10]. In all cases the binding isotherms can be fitted with a value of K_T of 0.02 in the absence of Ca^{2+} and of 0.2 in the presence of Ca^{2+}. These results are consistent with the proposal by Geeves & Halsall [5] that Tn/Tm controls myosin binding by controlling the isomerization between the two actomyosin states.

MATERIALS AND METHODS

Proteins

Myosin subfragment 1 (S1) was prepared by chymotryptic digestion of rabbit myosin [11]. F-actin was prepared by the method of Lehrer & Kerwar [12]. Pyrene-labelled actin (pyr-actin) was prepared as described previously [13].

Stopped flow

Rapid-mixing experiments were carried out in a Hi-Tech Scientific SF-3L or SF-51 stopped-flow spectrophotometer. Pyrene fluorescence was excited at 365 nm and emission was monitored through a KV393 glass filter. Signals from the photomultiplier were captured via an Infotech AD200 analogue-into-digital converter using a Hewlett–Packard 310 microcomputer. Data were analysed by using a non-linear least-squares routine [14].

Pressure relaxations

Pressure-relaxation equipment has been previously described [15]. Details of the use of equipment for inducing pressure relaxations in pyr-acto·S1 have been described by Coates *et al.* [7]. Pyrene fluorescence was monitored with an 1401 Intelligent Interface (Cambridge Electronic Devices) controlled from a Hewlett–Packard 310 microcomputer and analysed in the same way as for stopped-flow experiments.

Fluorescence titrations

Fluorescence titrations were carried out on a Perkin–Elmer LS-5B fluorescence spectrophotometer. Fluorescence was excited at 365 nm and emission was monitored at 407 nm; both fluorescence and emission used a 2.5 nm monochromator bandwidth. S1 was added to pyr-actin solutions by a continuous titrator built in the University of Bristol workshops. This delivered S1 at a rate of 4.1 μl/min to a continuously stirred cuvette. The efficiency of mixing was tested by titrating a fluorophore into a cuvette containing buffer; the resulting fluorescence was linearly dependent upon time and projected back to zero fluorescence at zero time. In all 400 data points were collected equally spaced over the time of a titration (typically 20 min) on an Epson PC AX2 microcomputer using software supplied by Perkin–Elmer.

Analysis of fluorescence titration data

The fluorescence signal (F) is related to the fractional saturation (α) of actin with S1 by:

$$\alpha = (F_0 - F)/(F - F_m)$$

where F_0 and F_m are the fluorescence values at [S1] = 0 and ∞ respectively. Titrations with uncontrolled pyr-actin were fitted to a hyperbola as described by Geeves [9]. Titrations with pyr-actin/Tn/Tm were fitted to a hyperbola as above or to the Geeves & Halsall model as follows. Pyrene fluorescence only gives a measure of S1 bound in the A·M state, and eqn. (1) describes the relationship between α and the free S1 concentration (M_F) for the Geeves & Halsall model.

$$\alpha = \frac{K_1 \cdot M_F(1 + K_1 \cdot M_F + K_1 \cdot K_2 \cdot M_F)^6 \cdot [K_T(1 + K_2)^7 + K_2]}{[K_T(1 + K_1 \cdot M_F + K_1 \cdot K_2 \cdot M_F)^7 + (1 + K_1 \cdot M_F)^7] \cdot (1 + K_2)^6} \quad (1)$$

$$M_T - M_F = \frac{A_T \cdot K_1 \cdot M_F \cdot [K_T(1 + K_2)(1 + K_1 \cdot M_F + K_1 \cdot K_2 \cdot M_F)^6 + (1 + K_1 \cdot M_F)^6]}{K_T(1 + K_1 \cdot M_F + K_1 \cdot M_F)^7 + (1 + K_1 \cdot M_F)^7} \quad (2)$$

The equation to relate M_F and the total concentration of actin (A_T) and S1 (M_T) was derived by Geeves & Halsall [5] and is given in a more convenient form in eqn. (2).

Fitting of binding isotherms was performed by a Monte Carlo method. Initial estimates of A_T, K_1, K_2 and K_T were supplied and eqn. (2) was solved by the Newton–Raphson iterative method to give a value of M_F for each M_T. The value of M_F obtained from this was then used to calculate α by using eqn. (1). The theoretical values of α were compared with the observed values and the sum of squares was calculated. The parameters were then randomly changed and the new parameters were tested for a better fit. This process was then repeated until the fit corresponded closely to the experiment data as judged by superimposition of the fitted and observed lines. The maximum random alteration of parameters was reduced after each unsuccessful attempt to improve the fit. Initial estimates of K_1 and K_2 for the fits came from the values obtained in the independent kinetic experiments. In order to decrease the time taken to arrive at the best fit not all parameters were allowed equal variability. The later half of the binding isotherm is defined by the overall association constant, which is $K_1(1 + K_2)$, and the early part by the relative size of K_2 and K_T. For most fits A_T was fixed and either K_1 or K_2 was fixed depending upon which constant was most accurately defined experimentally. The limitations of this routine are discussed after presentation of the data. The fitting program was written in Microsoft QuickBASIC and run on a Hewlett–Packard Vectra microcomputer.

RESULTS

Interaction of S1 with pyr-actin/Tn/Tm

Fig. 1 shows fluorescence titrations of pyr-actin with S1: each trace represents a computed average of three or four successive titrations. Fig. 1(*a*) is a titration with unregulated pyr-actin: the best fit to a binding isotherm for a single class of binding sites [9] is superimposed and gives $K_{ass.} = 6.7 \times 10^6\ M^{-1}$. This is in agreement with the value of $9.1 \times 10^6\ M^{-1}$ measured at slightly ionic strength [13]. Figs. 1(*b*) and 1(*c*) are titrations with the pyr-actin/Tn/Tm complex in the presence and in the absence of Ca^{2+} respectively. The binding isotherm in the absence of Ca^{2+} shows a distinct early lag phase. In the presence of Ca^{2+} the lag is less apparent. Under these conditions the theoretical line corresponding to the fitted parameters has only very slight co-operativity. The fitted parameters are, however, consistent with the results obtained by Greene [3] and with those obtained in the presence of nucleotides and nucleotide analogues (below). The titration shown in Fig. 1(*a*) and the control titrations described

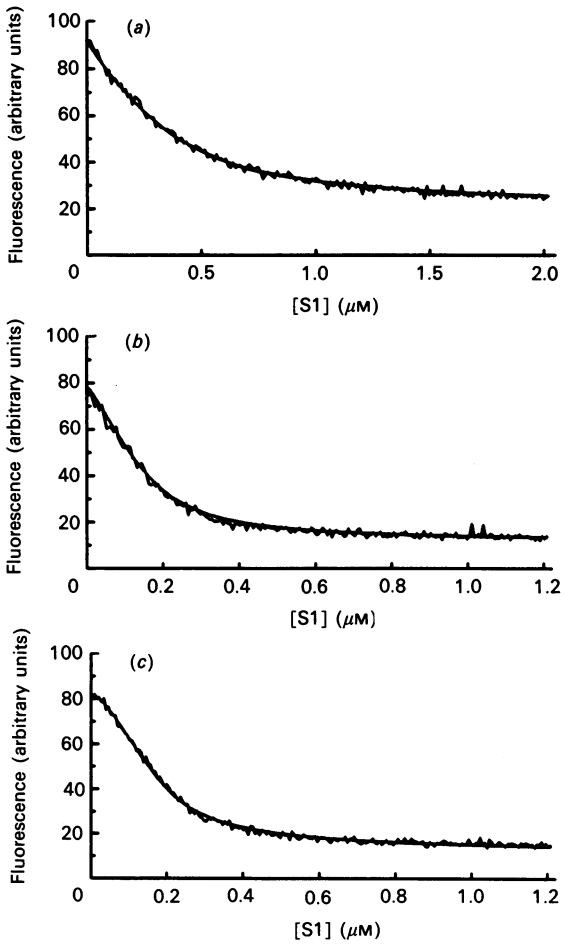

Fig. 1. Titration of pyr-actin with S1 monitored by pyrene fluorescence

(*a*) Binding of S1 to unregulated pyr-actin (0.2 μM). Fit to a single class of binding sites ($K_a = 6.7 \times 10^6$ M^{-1}) is shown superimposed. (*b*) Binding of S1 to 0.2 μM-pyr-actin + 0.11 μM-Tn/Tm + 1 mM-$CaCl_2$. Theoretical line corresponds to $K_1 = 1.3 \times 10^5$ M^{-1}, $K_2 = 222$ and $K_T = 0.16$. (*c*) Binding of S1 to 0.2 μM-pyr-actin + 0.11 μM-Tn/Tm + 1 mM-EGTA. Theoretical line corresponds to $K_1 = 1.3 \times 10^5$ M^{-1}, $K_2 = 168$ and $K_T = 0.009$. The buffer was 20 mM-Mops buffer, pH 7.0, containing 140 mM-KCl, 5 mM-$MgCl_2$ and 0.5 mM-dithiothreitol. All experiments were performed at 20 °C.

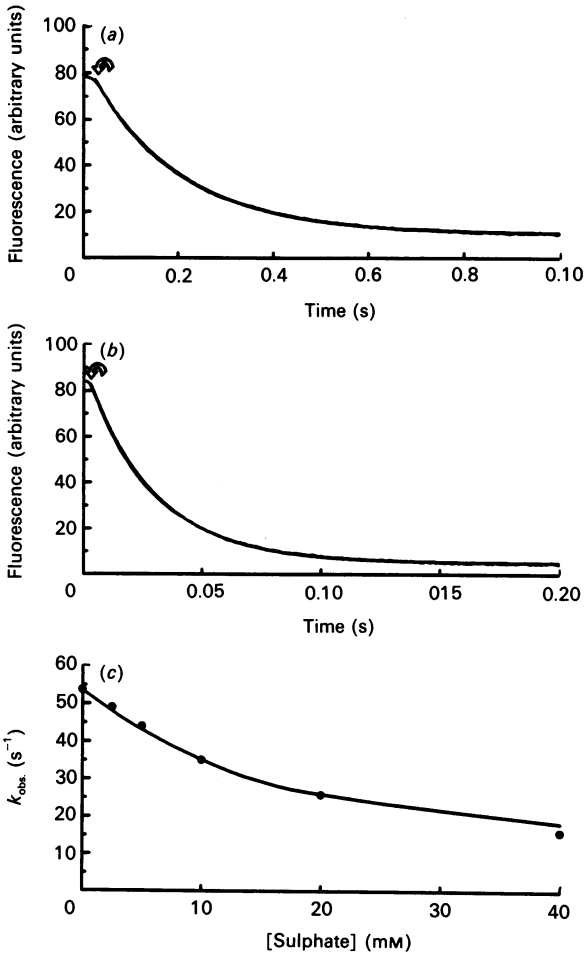

Fig. 2. Effect of sulphate on the ATP-induced dissociation of S1 from pyr-actin/Tn/Tm

Traces (*a*) and (*b*) are averages of five stopped-flow traces when 50 μM-ATP was rapidly mixed with 2 μM-S1. Arrows indicate the point at which the flow stopped. The buffer was as described in Fig. 1. (*a*) The observed rate constant was 53.7 s^{-1}. (*b*) Sulphate buffer (20 mM-Mops buffer, pH 7.0, containing 47 mM-K_2SO_4, 5 mM-$MgCl_2$ and 0.5 mM-dithiothreitol) was mixed with standard buffer to give a sulphate concentration of 10 mM. The observed rate constant was 35.1 s^{-1}. (*c*) Variation of $k_{obs.}$ with sulphate concentration. The fitted line gives a K_a for sulphate binding to pyr-acto/Tn/Tm·S1 of 18 mM.

in the Materials and methods section demonstrate that the lags seen in Figs. 1(*b*) and 1(*c*) are not due to inefficiency of mixing or to an error in defining the start of the titration. Similar binding isotherms have been reported to be obtained by using sedimentation methods [3,16]. The advantage of the method used here is that the binding is monitored continuously and therefore gives a greater definition to the overall binding isotherm.

In order to fit the binding isotherms to the Geeves & Halsall model [5], estimates of K_1 and K_2 need to be determined. The method of determining K_1 and K_2 has been described for unregulated acto·S1 [7] and used to measure K_1 and K_2 for regulated actin in the presence of Ca^{2+} [8]. These experiments were repeated under the experimental conditions used here and gave essentially the same result. As these experimental results have already been presented only the experimental approach is outlined here, and detailed results in the presence of sulphate are presented later below. Coates *et al.* [7] showed that pressure perturbs the equilibrium binding of actin to S1, and rapid changes in pressure induce two relaxations in pyr-acto·S1 (see Fig. 3). The fast phase occurs within the pressure-release time of the apparatus, and the slow phase can be fitted to a single exponential decay. The slow relaxation time is linearly dependent upon the free protein concentration, as defined by:

$$1/\tau_2 = k_{+1}([\bar{A}]+[\bar{M}])+k_{-1}/(1+K_2)$$

where $[\bar{A}]$ and $[\bar{M}]$ define the equilibrium concentrations of the proteins. The ratio of the amplitudes of the two relaxations (amp_1/amp_2) is also linearly dependent upon the free protein concentration:

$$amp_1/amp_2 = K_1([\bar{A}]+[\bar{M}])(1+K_2)/K_2+1/K_2$$

If $K_2 \gg 1$, then the slope defines K_1 and intercept $1/K_2$ (see Fig. 3*d*). The intercepts of the two plots are not well defined and K_2 cannot be determined. The dissociation rate constant $k_{-1}/(1+K_2)$ can be measured by the rate of displacement of pyr-actin/Tn/Tm from its complex with S1 by an excess of native actin/Tn/Tm (see Fig. 4). As k_{-1} can be calculated from k_{+1}/K_1 (defined by the gradients of the two plots), K_2 can be estimated from this displacement rate constant. The values of the rate and equilibrium constants obtained are shown in Table 1. These measurements

gave $K_1 = 1.3 \times 10^5$ M^{-1} and $K_2 = 204$ in the presence of Ca^{2+} and are in good agreement with the values previously reported at similar ionic strength and pH 7.5 [8].

The binding isotherms in Figs. 1(*b*) and 1(*c*) were fitted to the Geeves & Halsall model by the Monte Carlo method described above. K_1 is relatively well defined experimentally and was fixed at the value in Table 1, and the fitted curve defines K_2 and K_T. The fitted curve is superimposed in each case on the experimental data. The corresponding values for K_2 and K_T were 222 and 0.16 in the presence of Ca^{2+} and 168 and 0.009 in the presence of EGTA respectively. Thus the value of K_2 is in good agreement with that independently obtained from kinetic measurements in the presence of Ca^{2+}, and removal of the Ca^{2+} makes relatively little differences to its measured value. K_T in contrast is changed by a factor of 18-fold by Ca^{2+}. Thus the behaviour of the system is compatible with the Geeves & Halsall model. Geeves & Halsall [5] fitted data from Greene [3] using a value of 0.02 for K_T in the absence of Ca^{2+} at a similar ionic strength. If the Geeves & Halsall model is correct then repeating this experiment in the presence of an effector that changes K_1 and/or K_2 should yield the same values for K_T in the presence and in the absence of Ca^{2+}.

Interaction of pyr-acto/Tn/Tm·S1 in the presence of phosphate and sulphate

Both phosphate and sulphate have been shown to bind to the active site of S1 and compete with nucleotide binding [17,18]. McKillop & Geeves [10] have measured the effect of phosphate and sulphate binding on K_1 and K_2. Both anions reduced the overall affinity of S1 for actin by an order of magnitude, this involved a decrease in both K_1 and K_2.

The binding of phosphate and sulphate to pyr-acto/Tn/Tm·S1 was examined by their inhibition of the rate of dissociation of S1 from the complex with pyr-actin/Tn/Tm by ATP in the presence of Ca^{2+} (Figs. 2*a*–2*c*). Data were analysed according to eqn. (3) [19]:

$$k_{obs.} = \frac{k_0}{1+[L]/K_L} \quad (3)$$

where k_0 is the observed rate constant with no ligand added and K_L is the dissociation constant for the ligand with concentration [L]. This gave dissociation constants for phosphate and sulphate of 56 mM and 18 mM respectively. Values obtained with unregulated pyr-actin were 37 mM and 5.3 mM for phosphate and sulphate respectively [10]. Values for dissociation constants with S1 alone were determined from the effect of ligands on the binding isotherms of S1 and unregulated pyr-actin and were 1.2 mM and 0.9 mM for phosphate and sulphate respectively. These values are consistent with values published previously under different conditions [17,18]. Therefore, under the conditions of these experiments, S1 is more than 90% saturated with both ligands, and pyr-acto·S1 is 62% and 73% saturated with phosphate and sulphate respectively.

Equilibrium constants, K_1 and K_2, for the interaction of pyr-actin/Tn/Tm with S1 were determined in the presence of phosphate and sulphate as described above. The data are presented in Figs. 3 and 4 for sulphate, and the derived constants for both sulphate and phosphate are shown in Table 1. As complete saturation of acto·S1 with sulphate or phosphate was not possible at this ionic strength, the values shown in Table 1 are apparent values at the concentrations of ligand used. The

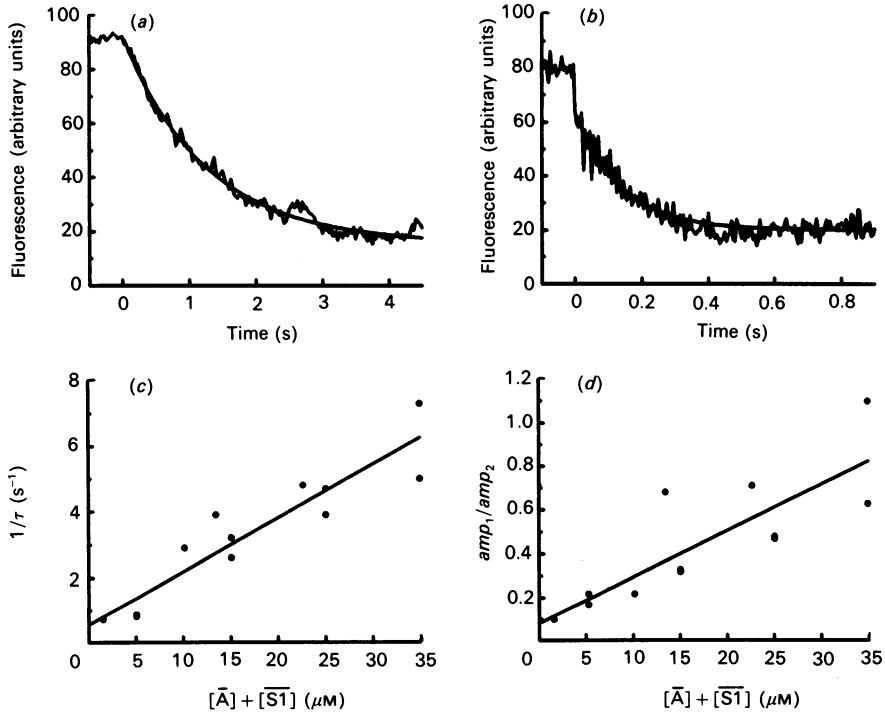

Fig. 3. Pressure-relaxation experiments on pyr-acto/Tn/Tm·S1 in the presence of sulphate

(*a*) and (*b*) At zero time pressure was released from 10.1 MPa to ambient pressure in 0.2 ms. Pyr-actin concentration was 5 μM and Tn/Tm concentration was 2.9 μM. S1 concentrations and values for $1/\tau$ were: (*a*) 10 μM and 0.8 s^{-1}; (*b*) 18.4 μM and 3.9 s^{-1}. (*c*) Variation of $1/\tau$ with free protein concentration. Linear least-squares regression gave a gradient of 1.6×10^5 M^{-1}·s^{-1}. (*d*) Variation of the amp_1/amp_2 ratio with free protein concentration. The data are from two separate experiments. In one of these actin alone gave a fast positive relaxation of 10 mV amplitude. The data from this experiment were corrected for this. Least-squares regression gave a gradient of 2.1×10^4 M^{-1}. The buffer was 20 mM-Mops buffer, pH 7.0, containing 47 mM-K_2SO_4, 5 mM-$MgCl_2$, 0.5 mM-dithiothreitol and 1 mM-$CaCl_2$.

relationship between the apparent value and the true value at saturating ligand is given by:

$$K_{1(app.)} = K_1(1 + K^A[L])/(1 + K^M[L])$$
$$K_{2(app.)} = K_2(1 + K^R[1])/(1 + K^A[L])$$

where K_1 and K_2 are the values in the absences of ligand and K^M, K^A and K^R are the association constants of the ligand for M, A–M and A·M respectively.

Fig. 5 shows fluorescence titration of pyr-actin/Tm/Tn in the presence of phosphate and sulphate. These isotherms show co-operativity both in the presence of Ca^{2+} (Figs. 5*a* and 5*c*) and in its absence (Figs. 5*b* and 5*d*), and it is therefore apparent that the presence of phosphate and sulphate produces binding isotherms that show clearer evidence of co-operativity than those in Fig. 1. The isotherms were fitted by using the Monte Carlo method with K_1 fixed at the value measured by the kinetic experiments (Table 1). Fitted values for K_2 and K_T are shown in Table 2, and the best-fit curves are superimposed on the data in Fig. 5. Once again the fitted value of K_2 is almost independent of the presence of Ca^{2+}, and the value is in good agreement with the value obtained in the kinetic experiment. The values of K_T show a 10-fold decrease on removal of Ca^{2+} in the presence of either phosphate or sulphate. The fitted values of K_T in the presence of sulphate are in good agreement with those obtained in the absence of added ligand, and those in the presence of phosphate are only 2-fold smaller.

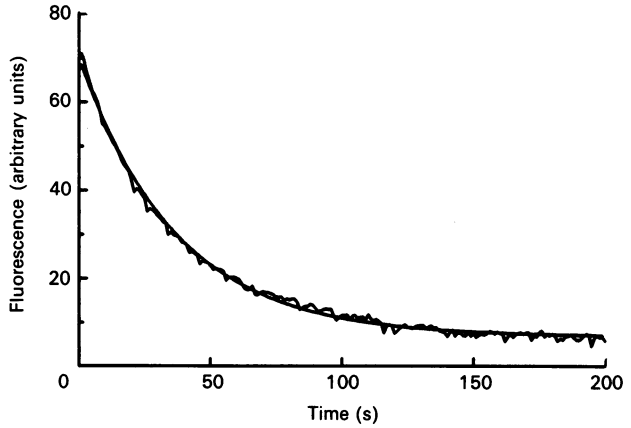

Fig. 4. Displacement of pyr-actin by excess native actin

Pyr-acto/Tn/Tm·S1 (10 μM) was mixed rapidly with 50 μM native actin/Tn/Tm. Trace is a average of five stopped-flow traces. The fitted line has an observed rate constant of 0.027 s^{-1}. The buffer was as described in Fig. 3.

Interaction of S1 with pyr-actin/Tn/Tm in the presence of ADP

In the presence of saturating amounts of ADP the affinity of S1 for unregulated actin is 1×10^6 M^{-1}; K_1 is, however, unchanged, whereas K_2 is decreased from 200 to 10 [9]. In the presence of ADP K_1 and K_2 cannot be measured by a pressure-relaxation experiment because, although the association of actin with M·ADP is still pressure-sensitive, the two relaxation times cannot be resolved. However, K_2 can be measured directly by measuring the fluorescence change that accompanied ADP binding to acto·S1 under conditions where no dissociation of the complex takes place. Under these conditions the fluorescence change observed is directly proportional to the fraction of acto·S1 occupying the A–M·D state [20]. By using this method, K_2 was estimated for pyr-acto/Tn/Tn·S1 in the presence of ADP and Ca^{2+} and gave a value of 18.

By using ADP inhibition of ATP-induced dissociation of acto·S1, the affinity of ADP for pyr-acto·S1 was measured as 150 μM and as 175 μM with pyr-acto/Tn/Tm·S1 (both in the presence of Ca^{2+}). This compares with a 170 μM for unregulated acto·S1 reported at pH 8 [21] and under similar conditions to

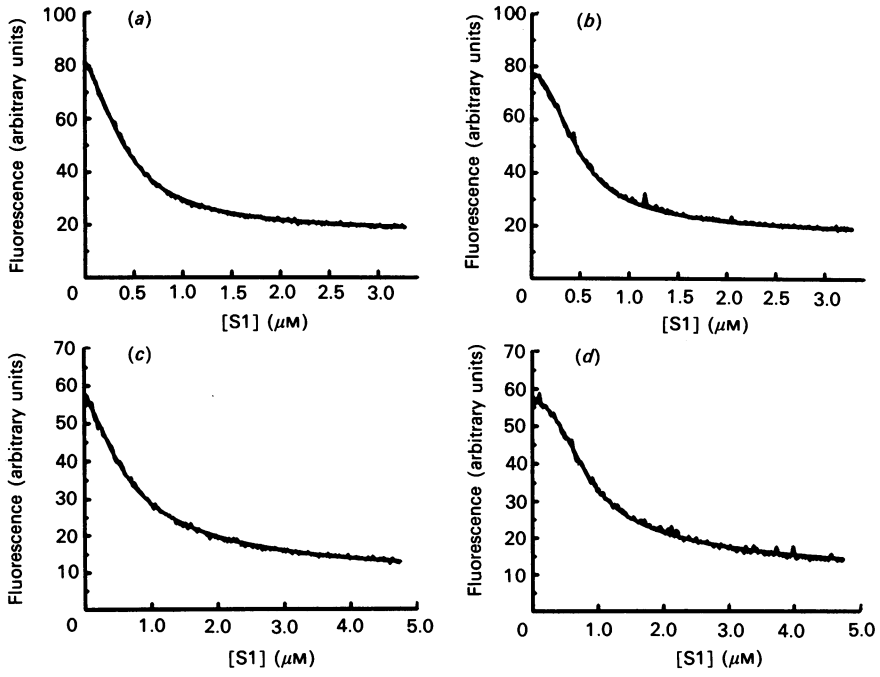

Fig. 5. Fluorescence titration of pyr-actin/Tn/Tm and S1 in the presence of phosphate and sulphate

S1 was added to 0.5 μM-pyr-actin + 4:7 Tn/Tm. Buffer was as Fig. 3 (*a* and *b*) or 90 mM-phosphate buffer, pH 7.0, containing 5 mM-$MgCl_2$ and 0.5 mM-dithiothreitol (*c* and *d*). Either 1 mM-$CaCl_2$ (*a* and *c*) or 1 mM-EGTA (*b* and *d*) was added. Traces are averages of a least three separate experiments. Theoretical lines correspond to the values in Table 2.

Table 1. Values of equilibrium and rate constants for the interaction of actin and S1

The values for phosphate and sulphate are apparent values at the concentrations of phosphate (90 mM) and sulphate (47 mM) used and are not saturating (see the text for discussion). Buffers were 20 mM-Mops buffer, pH 7.0, containing 5 mM-$MgCl_2$ and 0.5 mM-dithiothreitol with either sulphate or 140 mM-KCl added, or 90 mM-phosphate buffer, pH 7.0, containing 5 mM-$MgCl_2$ and 0.5 mM-dithiothreitol. The ADP concentration was 2 mM. The experiments were carried out at 20 °C.

Ligand	K_1 (M^{-1})	k_{+1} ($M^{-1} \cdot s^{-1}$)	k_{-1} (s^{-1})	$k_{-1}/(1+K_2)$ (s^{-1})	K_2
None	1.3×10^5	5.6×10^5	4.3	0.021	200
Phosphate	2.4×10^4	1.4×10^5	5.8	0.036	160
Sulphate	2.1×10^4	1.6×10^5	7.6	0.037	280
ADP	4.2×10^4	7.1×10^4	1.7	0.087	18

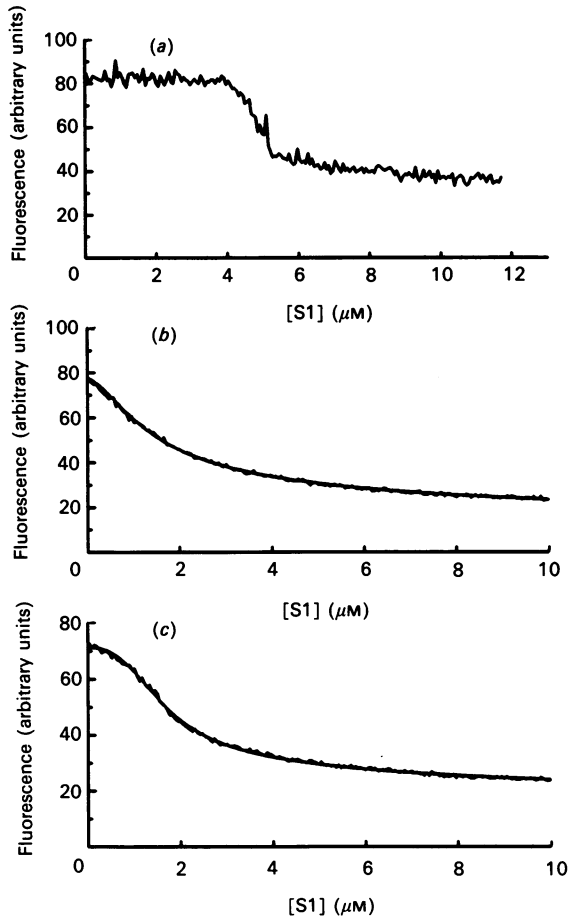

Fig. 6. Titration of pyr-actin/Tn/Tm and S1 in the presence of 2 mM-ADP

The buffer was as described in Fig. 1 with 50 μM-Ap_5A and 1 mM-$CaCl_2$ (*b*) or 1 mM-EGTA (*a* and *c*) added. Hexokinase (1 μM) and glucose (2 mM) were added to remove ATP in (*b*) and (*c*). (*b*) and (*c*) are averages of at least three experiments. Theoretical lines correspond to values given in Table 2.

those used here [9]. The dissociation rate was measured by using displacement of pyr-actin/Tn/Tm from its complex with S1·ADP by native actin/Tn/Tm in the presence of Ca^{2+} as described above. This gave an estimate of $k_{-1}/(1+K_2)$, which was used with the value of K_2 measured as above to calculate k_{-1} (Table 1). The first-order rate constant, k_{+1}, was measured from the concentration-dependence of the rate of association of pyr-actin/Tn/Tm with S1·ADP. This gave a straight line with slope $7.1 \times 10^4\ M^{-1} \cdot s^{-1}$. K_1 was calculated from k_{+1}/k_{-1} (Table 1).

The titration of S1 with actin in the presence of ADP is complicated by the contamination of ADP by ATP. ATP decreases the affinity of actin for S1 until there is sufficient ATPase activity to eliminate the contaminating ATP, and this can give rise to spuriously large co-operative binding. Pretreating the ADP with a trace of S1 and inclusion of Ap_5A in the titration was not sufficient to eliminate this problem (Fig. 6*a*). Addition of hexokinase and glucose to the titration removed the residual ATP and allowed the titrations shown in Figs. 6(*b*) and 6(*c*) to be collected. These isotherms were fitted to the model by using the measured value of K_2, which is more reliable than that for K_1 when ADP is bound. Again, the values of K_1 are independent of the presence of Ca^{2+} and are within a factor of 2-fold of the values measured in the kinetic experiment. The values of K_T are Ca^{2+}-dependent and are similar to the values produced from the fits to the earlier titrations.

DISCUSSION

The analysis of the binding isotherms for S1 binding to pyr-actin/Tn/Tm uses the measurements of K_1 and K_2 provided by the kinetic experiments. These measurements are independent of the detailed co-operative model, but do assume that the regulated actin filament is in the 'on' state when S1 is bound to the filament in the presence of Ca^{2+}. This assumption is fundamental to any co-operative model and is not a feature of this particular form of the model. If these measurements are made with fully switched-on thin filaments, then they are not complicated by the precise nature of the switched-off state. The values of K_1 and K_2 measured are consistent with previous measurements made in this laboratory with actin filaments [7,10,20,22] and reconstituted thin filaments [8]. The work presented here shows that Tm/Tn in the presence of Ca^{2+} causes a small increase in the affinity of actin for S1; the increase varies with the ligand bound to S1 and can be caused by an increase in K_1 (no ligand), in K_2 (ADP) or in both (phosphate and sulphate).

A problem in fitting the binding isotherms was the sensitivity of the fit to A_T, the parameter describing the initial concentration of actin monomers. Small variations in A_T caused marked variations in the fitted value of K_T. We were able to fit all the titration data in the absence of Ca^{2+} by using a fixed value of K_T of 0.02 and fitting A_T. This gave reasonable fits, with A_T varying by no more than 16% of the measured value. We therefore conclude that the model can be used to fit the data with values for K_T in the presence and in the absence of Ca^{2+} of 0.2 and 0.02 respectively.

A question arises as to the effect of incomplete saturation of pyr-actin/Tn/Tm·S1 with phosphate and sulphate, since the binding constants for phosphate and sulphate with pyr-acto/Tn/Tm·S1 and S1 indicate that there would be some dissociation of ligand from the S1 when it bound to pyr-actin/Tn/Tm. Full saturation of acto·S1 with ADP can be achieved, and the effect of partial saturation was examined at partially saturating ADP concentrations. The titrations fitted the model with the use of apparent K_1 and K_2 values. As the titrations in the presence of phosphate and sulphate were at the same ligand concentrations as the kinetic experiments, the apparent K_1 and K_2 values obtained are appropriate to describe the binding isotherm.

Analysis of the binding isotherms produced values of K_2 (K_1 for ADP) that were in good agreement with the experimentally determined values, the biggest discrepancy being a 2-fold difference in the presence of phosphate. As stated above, there is

Table 2. Values for the equilibrium constants describing the switching on of pyr-acto/Tn/Tm·S1 complex

An asterisk (*) denotes a parameter that was fixed during fitting at a value determined in Table 1. Conditions were as described in Table 1.

Ligand	K_1 (M^{-1})	K_2	K_T
None			
$+Ca^{2+}$	1.3×10^5*	220	0.17
$-Ca^{2+}$	1.3×10^5*	170	0.009
Phosphate			
$+Ca^{2+}$	2.4×10^4*	80	0.33
$-Ca^{2+}$	2.4×10^4*	70	0.025
Sulphate			
$+Ca^{2+}$	2.1×10^4*	300	0.2
$-Ca^{2+}$	2.1×10^4*	260	0.01
ADP			
$+Ca^{2+}$	3.3×10^4	18*	0.33
$-Ca^{2+}$	4.1×10^4	18*	0.02

a relatively large uncertainty in the estimated values of K_2, and a factor of 2-fold is not unacceptable. In all cases the fitted value of K_2 (K_1 for ADP) was independent of Ca^{2+}, the variation observed being within the experimental accuracy. Thus the model fulfils the first criterion of the model in that Ca^{2+} does not directly change the equilibrium constant of the A-to-R transition (K_2).

The fitted value of K_T is decreased by an order of magnitude on removal of Ca^{2+} under all of the conditions examined. The value of K_T is remarkably consistent under the different experimental conditions, giving a value of 0.17–0.33 in the presence of Ca^{2+} and 0.01–0.025 in its absence. This result is observed under conditions where the affinity of actin for S1 is varied by more than a factor of 10-fold; this is achieved by addition of sulphate or phosphate, which primarily changes K_1 with little effect on K_2, or addition of ADP, which alters K_2 with little change in K_1.

Thus the studies reported here are compatible with the earlier Hill *et al.* model [4] is that the thin filament is predominantly in the 'off' state even in the presence of Ca^{2+}; Ca^{2+} binding increases the fraction of the A_7·Tm·Tn units in the 'on' state from 2% to 20%. Binding of a strong S1 crossbridge is required to turn on an actin filament completely. The model used here, however, suggests that Tm can inhibit the isomerization of the acto·S1 complex from the A to the R state. This is a difference from the Hill *et al.* model [4] and the suggestion by Chalovich & Eisenberg [23] that Tm controls the phosphate-release step of the acto·S1 ATPase reaction. In the model of the ATPase proposed by Geeves *et al.* [6] the A-to-R transition is required before product release is accelerated by actin. Thus by controlling the A-to-R transition Tm can effectively control the release of phosphate, the transition from weak to strong actin affinity and the generation of force between actin and myosin in a muscle fibre. Geeves [24] has discussed in detail the relationship between the A-to-R transition, phosphate release, actin binding and force generation.

The model proposed is compatible with all of the published equilibrium studies that we have examined. These predict that approx. 80% of the thin filament is in an 'off' state in the presence of Ca^{2+} and that approx. 98% is in an 'off' state in the absence of Ca^{2+}. However, there is a discrepancy between these equilibrium studies and kinetic data. Studies by Trybus & Taylor [25], which have been repeated in this laboratory [26,27], show that the initial rate of S1 binding to thin filaments is faster in the presence of Ca^{2+} than in its absence. The results suggest that the rate of attachment of S1 to the thin filament is slower when the thin filament is switched off, and that the thin filament is predominantly in an 'off' state in the absence of Ca^{2+} but in a prodominantly 'on' state when Ca^{2+} is present. This is incompatible with the equilibrium estimates, which suggest that 80% of the thin filament is 'off' in the presence of Ca^{2+}.

The contradiction between the equilibrium and kinetic studies may be explained by the existence of two types of switched-off state, one with the properties of the 'closed' state described here and a further state that does not permit S1 attachment. Studies on the mechanics of single muscle fibres have lead to similar suggestions regarding the need for more than one regulatory step [28,29]. We are currently attempting to characterize this additional state and the relationship between this and the 'closed' state. The equilibrium data described here can be fitted by a model that incorporates an additional class of 'off' state and retains the characteristics of the Geeves & Halsall model that are necessary to explain the co-operativity in the presence of Ca^{2+} and the dependence of this co-operativity on nucleotide.

The interpretation of the results presented here is based on the assumption that the co-operative unit comprises seven actin monomers and one tropomyosin molecule. Other types of co-operative interaction are possible, for example nearest-neighbour interactions between actin monomers along the thin filament [30]. These models do not exclude the essential property of the Geeves & Halsall model, namely that tropomyosin controls the isomerization of the actomyosin complex. The lack of co-operativity in the absence of tropomyosin clearly implicates tropomyosin in the regulatory process, and an A_7·Tm co-operative unit remains an attractive structural model.

The model proposed by Geeves & Halsall [5] and supported by the experimental data described here suggests that Tm controls the acto·S1 interaction by controlling the isomerization of the acto·S1 complex. The nature of the acto·S1 isomerization is not known and may involve changes in the S1 head, the acto·S1 interface, the actin monomer alone or a combination of these. It is difficult to see how TM could regulate a change that involved the S1 head alone; however, Tm regulation of the isomerization is easily compatible with an isomerization that involves actin alone or the acto·S1 interface. For example, if the isomerization involved a transition from a one-site attachment to an attachment at a second point, then tropomyosin could block this transition in the 'closed' state (see ref. [31]). The 'closed' and 'open' states exist in the absence of troponin [32], and a simplest explanation of the action of troponin would be as modulator of the equilibrium between the two thin-filament states.

These studies do not address the problem of the contribution of tropomyosin end-to-end interactions to the thin-filament co-operativity. We have successfully fitted the isotherms obtained without reference to such interactions. However, this does not rule out the possibility that end-to-end interactions occur and are being compensated for by a lower value of K_T. Pan *et al.* [16] studied this question by measuring the co-operative binding of S1 to thin filaments assembled from native tropomyosin and Tm with the 11 *C*-terminal residues removed. The truncated Tm would be expected to have a diminished end-to-end interaction. Fitting their results to the Hill *et al.* model [4] gave $L = 34$ and $Y = 7$ for native Tm and gave $L = 77$ and $Y = 1$ for truncated Tm with no change in the affinity of S1 for the modified thin filament. This analysis is compatible with the modified Tm abolishing co-operativity due to end-to-end interactions and increasing the co-operativity within a single Tm unit. Fitting their data to our model gave a good fit with $K_T = 0.011$ (i.e. $1/K_T = 91$, equivalent to L) for native Tm whereas the data for modified Tm required a lower affinity of S1 for the filament and $K_T = 0.026$ ($1/K_T = 38$). Thus the model presented here suggests

that the modification of Tm decreases the co-operativity by increasing K_T (decreasing L) and decreasing K_1. This interpretation is not unreasonable, as the binding of Tm to actin increases K_1. Thus either interpretation is compatible with the experimental data, so we believe that the analysis of binding isotherms cannot be used to demonstrate the role of end-to-end interactions between Tm molecules in thin filament co-operativity.

We thank H. Gutfreund and D. Halsall for comments on this manuscript. This work was supported by the Wellcome Trust. M. A. G. is a Royal Society University Research Fellow.

REFERENCES

1. Ebashi, S. & Ebashi, F. (1964) J. Biochem. (Tokyo) **55**, 604–613
2. Greene, L. E. & Eisenberg, E. (1980) Proc. Natl. Acad. Sci. U.S.A. **77**, 2616–2620
3. Greene, L. (1982) J. Biol. Chem. **257**, 13993–13999
4. Hill, T. L., Eisenberg, E. & Greene, L. (1980) Proc. Natl. Acad. Sci. U.S.A. **77**, 3186–3190
5. Geeves, M. A. & Halsall, D. J. (1987) Biophys. J. **52**, 215–220
6. Geeves, M. A., Goody, R. S. & Gutfreund, H. (1984) J. Muscle Res. Cell Motil. **5**, 351–361
7. Coates, J. H., Criddle, A. H. & Geeves, M. A. (1985) Biochem. J. **232**, 352–356
8. Geeves, M. A. & Halsall, D. J. (1986) Proc. R. Soc. London B **229**, 85–95
9. Geeves, M. A. (1989) Biochemistry **28**, 5864–5871
10. McKillop, D. F. A. & Geeves, M. A. (1990) Biochem. Soc. Trans. **18**, 585–586
11. Weeds, A. G. & Taylor, R. S. (1975) Nature (London) **257**, 54–57
12. Lehrer, S. S. & Kerwar, G. (1972) Biochemistry **11**, 1211–1217
13. Criddle, A. H., Geeves, M. A. & Jeffries, T. (1985) Biochem. J. **232**, 343–349
14. Edsall, J. T. & Gutfreund, H. (1983) Biothermodynamics, pp. 228–236, John Wiley and Sons, New York
15. Davis, J. S. & Gutfreund, H. (1976) FEBS Lett. **72**, 199–207
16. Pan, B.-S., Gordon, A. M. & Luo, Z. (1989) J. Biol. Chem. **264**, 8495–8498
17. Bagshaw, C. R. & Trentham, D. R. (1974) Biochem. J. **141**, 331–349
18. Tesi, C., Barman, T. & Travers, F. (1988) FEBS Lett. **236**, 256–260
19. Siemankowski, R. F. & White, H. D. (1984) J. Biol. Chem. **259**, 5045–5053
20. Geeves, M. A. & Jeffries, T. E. (1988) Biochem. J. **256**, 41–46
21. White, H. D. (1977) J. Biophys. **17**, 40a
22. Geeves, M. A., Jeffries, T. E. & Millar, N. C. (1986) Biochemistry **25**, 8454–8458
23. Chalovich, J. M. & Eisenberg, E. (1982) J. Biol. Chem. **257**, 2432–2437
24. Geeves, M. A. (1991) Biochem. J. **274**, 1–14
25. Trybus, K. M. & Taylor, E. W. (1980) Proc. Natl. Acad. Sci. U.S.A. **77**, 7209–7213
26. Halsall, D. J. (1987) Ph.D. Thesis, University of Bristol
27. McKillop, D. F. A. (1991) Ph.D. Thesis, University of Bristol
28. Babu, A. Gulati, J. (1988) Adv. Exp. Med. Biol. **266**, 101–112
29. Payne, M. R. & Rudnick, S. E. (1989) Trends Biochem. Sci. **14**, 357–360
30. Balazs, A. C. & Epstein, I. R. (1983) Biophys. J. **44**, 145–151
31. Milligan, R. A. & Flicker, P. F. (1987) J. Cell Biol. **105**, 29–39
32. Ishii, Y. & Lehrer, S. S. (1990) Biochemistry **29**, 1160–1166

Received 19 April 1991/14 May 1991; accepted 21 May 1991